

Functional and structural characterization of ovine ornithine transcarbamoylase †

Ambra De Gregorio,^a Roberto Battistutta,^{b,e} Nicoletta Arena,^a Manuela Panzalorto,^c Pietro Francescato,^b Giovanna Valentini,^d Giuseppe Bruno^c and Giuseppe Zanotti^{*b,e}

^a Department of Organic and Biological Chemistry, University of Messina, Salita Sperone 31, 98166 Messina, Italy

^b Department of Organic Chemistry, University of Padova and Biopolymer Research Center, Consiglio Nazionale delle Ricerche, 35131 Padova, Italy

^c Department of Inorganic, Analytical, and Physical Chemistry, University of Messina, Salita Sperone 31, 98166 Messina, Italy

^d Department of Biochemistry "A. Castellani", University of Pavia, Via Taramelli 31B, 27100 Pavia, Italy

^e Venetian Institute of Molecular Medicine, VIMM, Via Orus 2, Padova, Italy

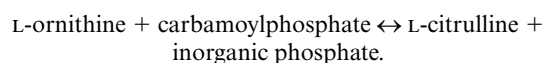
Received 6th May 2003, Accepted 7th August 2003

First published as an Advance Article on the web 20th August 2003

Ornithine transcarbamoylase from ovine liver has been purified to homogeneity. Like all anabolic OTCs, the ovine enzyme is a trimer, constituted by identical subunits of 34 kDa. Sequence analysis of the 54 N-terminal residues of ovine OTC shows a high degree of homology with the human enzyme. The optimum pH and the Michaelis constants for the catalytic reaction were determined. The ovine enzyme is the most thermostable one among mammals OTCs, its critical temperature being 6 °C higher than those measured for the other enzymes. The enzyme has been crystallised and the structure determined at 3.5 Å resolution. Crystals belong to the cubic $P4_32$ space group, with $a = b = c = 184.7$ Å and a solvent content of about 80%. There is no evidence of any ligand in the active site cavity, indicating that the crystals contain an unliganded or T state of the enzyme. The unliganded OTCase enzyme adopts a trimeric structure which, in the crystal, presents a three-fold axis coincident with the crystallographic one. The conformation of each monomer in the trimer is quite similar to that of the liganded human protein, with the exception of a few loops, directly interacting with the substrate(s), which are able to induce a rearrangement of the quaternary organisation of the trimer, that accounts for the cooperative behaviour of the enzyme following the binding of the substrates.

Introduction

Ornithine transcarbamoylases (OTCases, EC 2.1.3.3) catalyse the reaction:



Anabolic OTCase is an ubiquitous enzyme that catalyses the carbamoylation of L-ornithine to form L-citrulline in both the L-arginine biosynthesis and the urea cycle. In bacterial cells a catabolic OTCase can also be present, which participates in anaerobic degradation of L-arginine. The protein has been isolated from several species, from bacteria to mammals, and in all cases it is made up of a polypeptide chain of 34–36 kDa, which generally assembles in a trimeric form to make the anabolic enzyme, and in a more complex organisation to constitute the catabolic enzyme. In anabolic OTCases each polypeptide chain folds into two domains, a carbamoylphosphate binding domain (polar domain) and an L-ornithine binding domain (equatorial domain). OTCases are conservative enzymes as demonstrated by the fact that the human OTCase¹ shows a high sequence homology with the *E. coli* OTCase^{2,3} and both enzymes with the catalytic subunit of the closely related enzyme aspartate transcarbamoylase (ATCase, EC 2.1.3.2.)^{4,5} of the same micro-organism, leading to the hypothesis of a common origin for transcarbamoylases.

The crystal structure of several bacterial species of the transcarbamoylase family is known, the prototype of which is the ATCase from *E. coli*.⁶ In addition, the structures of the catabolic OTCase from *Pseudomonas aeruginosa*,⁷ of the anabolic OTCase from *Pyrococcus furiosus*,⁸ and of anabolic OTCase from *E. coli*^{9,10} have been determined. The two first bacterial OTCases previously mentioned are dodecamers, whilst the OTCase from *E. coli* is a trimer. Recently, the molecular model of human OTCase complexed with the bi-substrate analogue δ -N-phosphonacetyl-L-ornithine (δ -PALO)¹¹ and with carbamoylphosphate¹² has been obtained.

The quaternary organisation of these enzymes is particularly relevant to its cooperative behaviour: kinetic and spectroscopic data suggest that the trimeric OTCase undergoes a conformational transition upon binding of carbamoyl phosphate, reaching a more stable three-dimensional structure.^{13,14} The human enzyme has been crystallised in two different states: in the presence of a bi-substrate analogue, in a conformation which is assumed to be an R state, and in the presence of only one of the two substrates, carbamoylphosphate, in a state that is possibly intermediate between the R and the T states. At present, the structure of an eukariotic trimeric OTCase in the T state is not yet available.

With the aim of improving the understanding of the conformational changes which the anabolic OTCase undergoes upon substrates binding, a study was undertaken to determine the crystal structure of ovine OTCase in the T state. In this paper, we present the crystal structure at low resolution of the unbound ovine liver OTCase and its functional characterisation.

† Electronic supplementary information (ESI) available: a Ramachandran plot, and two figures illustrating statistics on the geometrical parameters of the structure. See <http://www.rsc.org/suppdata/ob/b3/b304901a/>

Table 1 Michaelis constants of ovine OTCase for carbamoyl phosphate and ornithine at various pH values. Ornithine carbamoyl-transferase activity was determined in the Experimental section. The buffer was diethanolamine/MES/N-ethylmorpholine (0.051 M/0.1 M/0.051 M)

pH	8.2	8.6	9.0
K_m L-ornithine	0.33	0.25	0.45
K_m carbamoyl-P	0.087	0.033	0.25

Results and discussion

Enzyme purification

The ovine liver OTCase was purified to homogeneity with a rapid and simple procedure including two affinity chromatography steps on the transition-state analogue δ -PALO covalently bound to Sepharose 6B. The purified enzyme showed a specific activity of 508 U mg⁻¹, which is in the middle of the values already reported for mammalian OTCases, *i.e.* 233 and 211 U mg⁻¹ for human¹⁵ and dolphin¹⁶ enzymes, and 780 and 870–920 for bovine¹⁷ and rat¹⁸ enzymes, respectively. Typically, activity yields were in the range of 40–45% and the enzyme obtained from 1 g of liver tissue was *ca.* 55–60 μ g.

Criteria of homogeneity

The homogeneity of the purified enzyme was checked either by PAGE in the absence and in the presence of SDS or by N-terminal sequence analysis (see below). In each case, only a single species protein was appreciated.

Molecular characterization

The purified enzyme, analyzed according to the procedure of Leammly¹⁹ on a SDS 12% PAGE, migrated as a protein of molecular mass of about 34 kDa. The enzyme submitted to size-exclusion chromatography on Sephacryl S-200 column eluted at a position of 102 kDa, as a single peak, symmetric in shape (data not shown). Taken together, these results show that the ovine OTCase approaches the trimer form, the same oligomeric structure previously reported for other mammalian sources.^{20,18}

pH optimum of the reaction

In diethanolamine/MES/N-ethylmorpholine tri-buffer over the pH range from 7.0 to 9.4, a bell-shaped activity curve was observed, the pH optimum varying with the L-ornithine concentration. At 10 mM L-ornithine the optimum was pH 8.2, while when the ornithine concentration was lowered up to 0.025 mM the pH optimum shifted to 8.6. These results confirm that: (i) only the minor zwitterionic species of ornithine, H₂N(CH₂)₃-CH(NH₃⁺)COO⁻, is the substrate of the enzyme,²¹; and (ii) a relatively high concentration (10 mM) of the above substrate inhibits the ovine OTCase, as already observed for the human enzyme.²²

Kinetic studies

The Michaelis constants (K_m) of ovine OTCase were determined for both carbamoylphosphate and ornithine at pH values of 8.2, 8.6, and 9.0, at fixed 10 mM substrate. The double reciprocal plot of velocity *versus* concentrations of the variable substrate (10–0.01 mM and 10–0.05 mM for carbamoylphosphate and ornithine, respectively) was used to obtain K_m values. As shown in Table 1, the apparent K_m values of ovine OTCase for carbamoylphosphate and ornithine at different pHs ranged from 0.25 to 0.033 and from 0.45 to 0.25, respectively, which are similar to K_m s of the human,¹⁵ rat,¹⁸ and

Table 2 Half inactivation times (min) of ovine OTCase subjected to heat treatment in the absence and in the presence of 20 mM ligands (L-ornithine: ORN; L-norvaline: NOR; carbamoyl-P: CP).

50 °C no addition	55 °C no addition	63 °C CP	63 °C ORN	63 °C CP + NOR
41	16	15	3	stable

bovine¹⁷ liver enzymes. Although it must be emphasized that, at pH 8.6, high concentrations of ornithine exhibited an inhibitory effect, at that same pH value we observed the highest affinity of the enzyme towards the substrates.

Thermal inactivation

Ovine OTCase is the most thermostable one among mammal OTCases its critical temperature being 63 °C, which is about 6 °C higher than those measured for human²³ and dolphin¹⁶ enzymes. The higher thermostability of ovine enzyme compared to that of other mammal OTCases could be due to a greater number of hydrophobic interactions and/or ion pairs, which usually stabilize the enzyme conformation. Ovine OTCase is protected from thermal inactivation by substrates and/or analogues binding (Table 2). At the critical temperature of 63 °C, the presence of carbamoylphosphate or inorganic phosphate appreciably increases the half-life of the enzyme ($t_{1/2}$ = 15 and 7.5 min, respectively), while L-ornithine or L-norvaline have only a slight stabilizing effect ($t_{1/2}$ = 3 and 1.5 min, respectively). This behavior confirms the attainment of conformational change upon formation of enzyme–carbamoylphosphate or enzyme–inorganic phosphate binary complex.¹⁴ When phosphate and L-ornithine are both present the half-life of the enzyme increases ($t_{1/2}$ = 42 min), but the strongest protective effect is observed in the presence of carbamoylphosphate and L-norvaline. This fact confirms that stabilizing changes of enzyme conformation take place during the formation of the carbamoylphosphate-L-ornithine–enzyme ternary complex.^{11,12}

Protein sequencing

Edman degradation of the purified OTCase (300 pmol monomer) provided us with a sequence of the first 54 amino acid residues. The extended N-terminal sequence that we obtained not only shows the high degree of homology of ovine OTCase with corresponding mammal enzymes, but also works to highlight the high level of homogeneity of the enzyme preparation. The alignment of this sequence with that from the human enzyme shows an absolute identity, apart for the first amino acid residue. Therefore, on the whole, these findings together with the thiol groups analysis (see below) supported us in using the human sequence in building the molecular model in the crystal structure.

Thiol groups analysis

It is known that disulfide bonds help proteins in stabilizing their conformation and holding out against heat inactivation. Therefore, to gain some understanding of the heat stability exhibited by ovine OTCase (see below), we undertook the chemical modification of free and total thiol groups of the enzyme (see the Materials and methods section). Reaction of the protein (240 μ g) with Ellman's reagent (5,5'-dithiobis(2-nitrobenzoic acid) (DTNB) in the presence of 8M urea resulted in titration of 2.93 nmol cysteine residue per nmol monomer. Treatment of the protein (340 μ g) with labeled (14C) iodoacetic acid, followed by trypsin digestion, separation and identification of labeled peptides containing S-carboxymethylate cysteine groups, allowed to infer that ovine OTCase contains a total amount of 3 cysteine residues. As 3 free cysteine residues have been detected by analysis with DTNB, taken together these

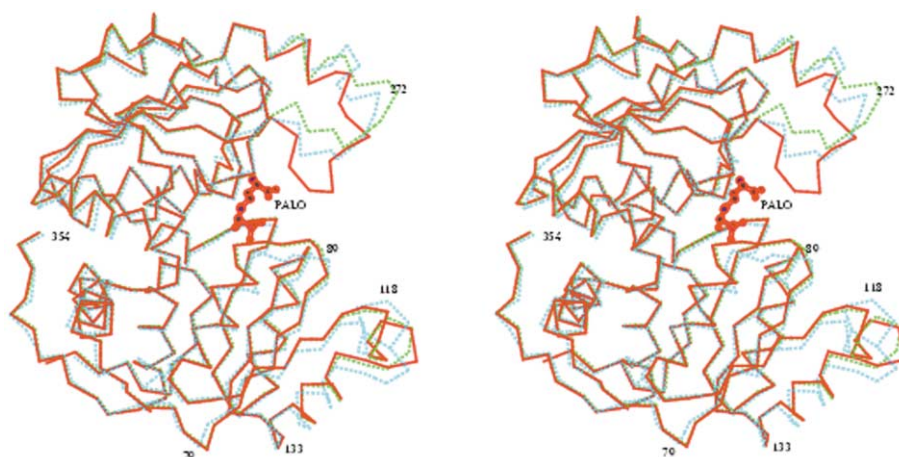


Fig. 1 Superposition of Ca chain trace of the monomer of ovine OTCase (dashed light blue line) to the corresponding Ca trace of human OTCase bound to PALO (red line;¹¹) and to carbamoylphosphate (dashed green line;¹²). δ -PALO, as it is bound to the human protein, is shown in ball and sticks. Significant differences are observed in regions 87–95, 105–124 and 264–282. The area of the monomer that interacts with another monomer in the trimer and where we observe a spurious density is close to residues 79 and 133 (see text for details).

results suggest that: (i) like in human enzyme, 3 are the cysteines present in ovine OCTase; (ii) no one cysteine is engaged in disulfide bridge; (iii) the 3 free cysteines can not account for the higher heat stability exhibited by ovine OCTase.

Crystal structure

Structure of the monomer. The tertiary structure of the ovine OTCase monomer is similar to that of the human protein complexed with δ -PALO¹¹ and carbamoylphosphate¹² and to that of other bacterial transcarbamoylases^{6–8,10,24} (Fig. 1). Superposition of Ca atoms of our model with those of the human protein (PDB ID 1OTH) gives a root mean square deviation of 1.40 Å, that drops to 0.56 Å if a few zones, significantly different, are not considered in the calculation. In particular, amino acids from 87 to 95 are displaced by *ca.* 3 Å from the position they occupy in the human protein. The loop containing amino acids from 305 to 307 is also slightly affected by the absence of the ligand in the active site. Other two zones present a different conformation in the unliganded protein and are strongly influenced by the absence of a ligand in the active site: residues from 110 to 124 and from 264 to 282. Both regions are apparently quite flexible in our model and in some part they are positioned tentatively. In the portion 116–122, since only the main chain is visible in the electron density map, alanine residues were fitted instead of the human amino acid sequence. All the above mentioned regions contain residues that are involved in the binding of the substrate or substrate analogue.^{11,12}

The substrates binding cavity, located in-between the two domains, is empty in our model, despite the fact that the protein was purified in the presence of small amounts of carbamoylphosphate, inorganic phosphate and L-norvaline. The two latter compounds are competitive inhibitors of carbamoylphosphate and of the other co-substrate, L-ornithine, respectively.²⁵ All these ligands were not introduced in the precipitant solution during the crystallization experiments and we do not know the exact concentration of these small molecules in the starting solution, since they were diluted during the concentration of the protein (see Experimental section). Moreover, carbamoylphosphate is unstable in solution at room temperature and it could easily be degraded during crystal growth at room temperature and eventually during the few weeks elapsed between data collection. Consequently, despite the fact that the initial concentration of carbamoylphosphate in the drops was 10 mM, its final concentration at the time of the crystal measurements is likely to be negligible. The only density clearly visible in the Fourier-difference electron density map was close to residues 79 and 133, *i.e.* at the interface between subunits in the trimer. At

this resolution it appears impossible to decide unequivocally about this density, but it appears likely that residue 133 is a larger amino acid than the Ser in the human protein. In bacterial OCTases, residue 133 is in fact an arginine.

Structure of the trimer. The superposition of the Ca atoms of the trimer of ovine OTCase and the human protein complexed with δ -PALO and carbamoylphosphate is shown in Fig. 2A and B. When one monomer of the human liganded OTCase is superimposed on a monomer of the ovine unliganded protein, the other two monomers in the trimer present a distance from the corresponding Ca atoms which reaches a maximum of about 8 Å. In fact, the two trimers differ significantly in their quaternary structure, that of the unliganded protein being more “opened” with respect to the two liganded ones. The displacement can be evaluated in about 14° in a direction perpendicular to the ternary axis of the trimer. A similar situation can be observed in the anabolic enzyme from *E. coli*, but in that case the relative movement of the subunits is less pronounced. The difference we observe between the two trimers cannot be ascribed to uncertainty in our model due to the low resolution, since only one monomer is present in the asymmetric unit and in both structures, ovine and human, the trimer is formed by a crystallographic symmetry operation. As previously pointed out, the monomer itself is similar in the two proteins, except for a few regions involved in the interaction with δ -PALO or carbamoylphosphate. Differences in the quaternary organization of the trimer correspond to structural differences in the arrangements of the monomers in the trimer. The contacts between monomers are summarized in Table 3, where residues of two monomers that have atoms at a distance shorter than a given value are listed, both for the ovine unliganded and for human liganded protein. Despite the low resolution of the model, it is evident that the different arrangements of the monomers give rise to significant changes in the interactions.

Implications for cooperativity. The proposed mechanism of activation of the enzyme, based on biochemical data, indicates that carbamoylphosphate binds first to the active site and induces a large conformational modification.¹⁴ Then ornithine, the second co-substrate, binds and induces a second conformational change.¹³ The differences observed in the quaternary structures of mammalian OCTases perfectly agree with this behaviour. In fact, the major difference in quaternary structure is observed between the ovine unliganded and the human carbamoylphosphate liganded enzyme,¹² that can be described as a rotation of 14° with respect to the three-fold axis. The binding of δ -PALO, that partially mimics the presence of the

Table 3 Inter-subunit contacts within the OTCase trimer. Amino acids that have at least one atom at a distance less than 3.5 Å from a residue of the symmetry related molecule in the trimer are reported. Columns 1 and 2 are relative to the liganded human enzyme (PDB code 1OTH), columns 4 and 5—to the ovine unliganded enzyme (this work)

δ-PALO Human liganded OTCase			Ovine unliganded OTCase		
Residue 1	Residue 2	Distance/Å	Residue 1	Residue 2	Distance/Å
Gly79 O	Leu103 Cδ1	3.5	Gln78 Oε1	Tyr73 Cδ2	3.4
His107 Nε2	Glu98 Oε2	2.8	His107 Nη2	Glu98 Oε1	2.9
			His107 Cγ	Ala102 Cβ	3.4
Cys109 Sγ	Glu98 Oε1	3.4	Cys109 Sγ	Glu98 Oε2	3.5
Phe110 O	Arg94 NH2	2.9	Phe110 O	Arg94 NH2	2.2
Thr113 O	Arg89 NH1	2.6	Thr113 Oγ1	Arg89 NH2	3.2
			Gln114 Oε1	Arg89 NH2	2.9
			Gln114 Cγ	Thr91 Cβ	3.3
			Gln114 Nε2	Arg94 NH1	3.3
Asp115 O	Arg89 Cα	3.3			
Asp115 O	Ser90 N	2.9			
Ile116 O	Arg89 NH1	2.9			
His117 N	Thr91 Oγ1	3.1			
His117 Cδ2	Arg92 NH2	3.4			
Glu122 Oε2	Arg92 NH1	2.7			
Asp126 Oδ1	Tyr317 OH	2.9			
Asp126 Oδ1	Phe324 Cζ	3.5	Asp126 Oδ1	Tyr317 OH	3.2
Met134 Cε	Ala327 O	3.2	Met134 Cγ	Leu95 Cδ2	3.3
Met134 O	Lys331 Nζ	2.9	Met134 O	Lys331 Nζ	2.9

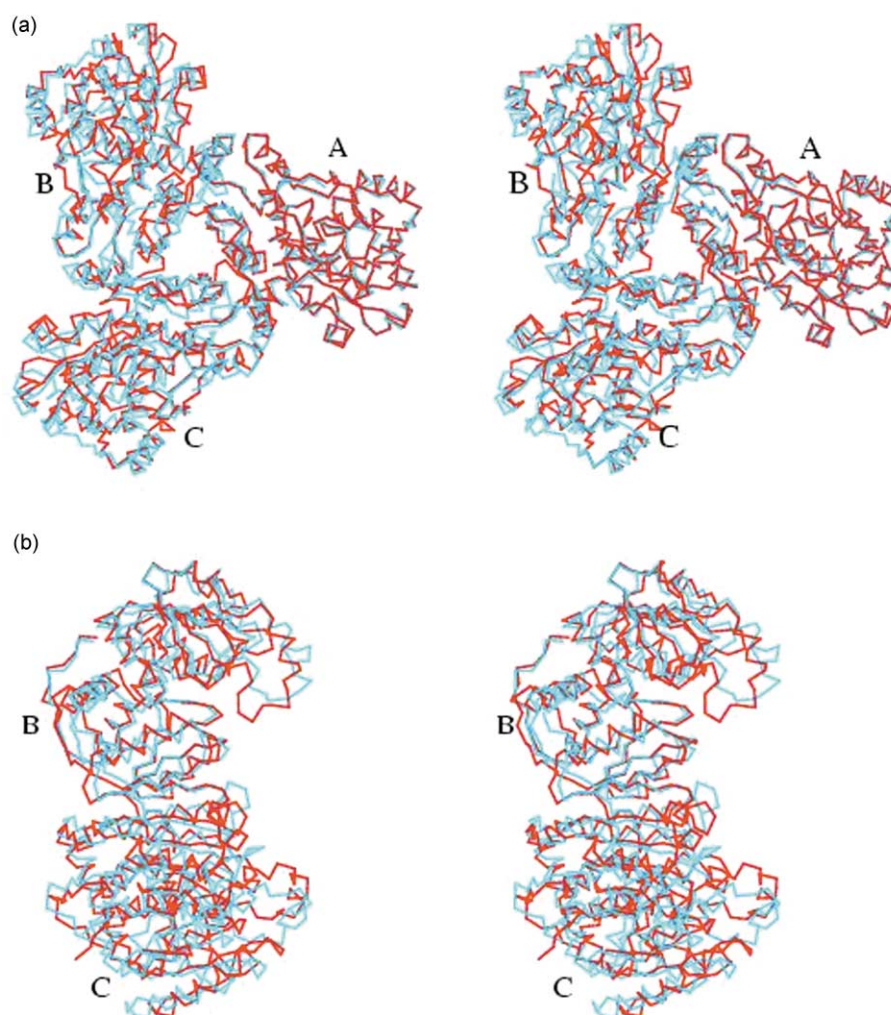


Fig. 2 (A) Superposition of Ca atoms of the ovine OTCase trimer (blue) with the corresponding Ca atoms of human liganded OTCase (red; PDB code 1OTH). The trimer is drawn approximately down the three-fold axis. Comparison was made using the transformation matrix that produces the better superposition of monomers A of the two molecules and transforming the other two monomers, B and C, using the same matrix. (B) Same as (A), rotated by 90° with respect to the previous view. For clarity, only monomers B and C, *i.e.* those oriented in a different way in the trimer, are shown.

two substrates, induces another minor rotation that has been estimated in other 3–4°.¹²

The major reason for this movement seems to be the presence

of a substrate or a pseudo-substrate in the active site cavity, that induces some defined conformational modifications and fixes some flexible loops, and in doing so it stabilises an active

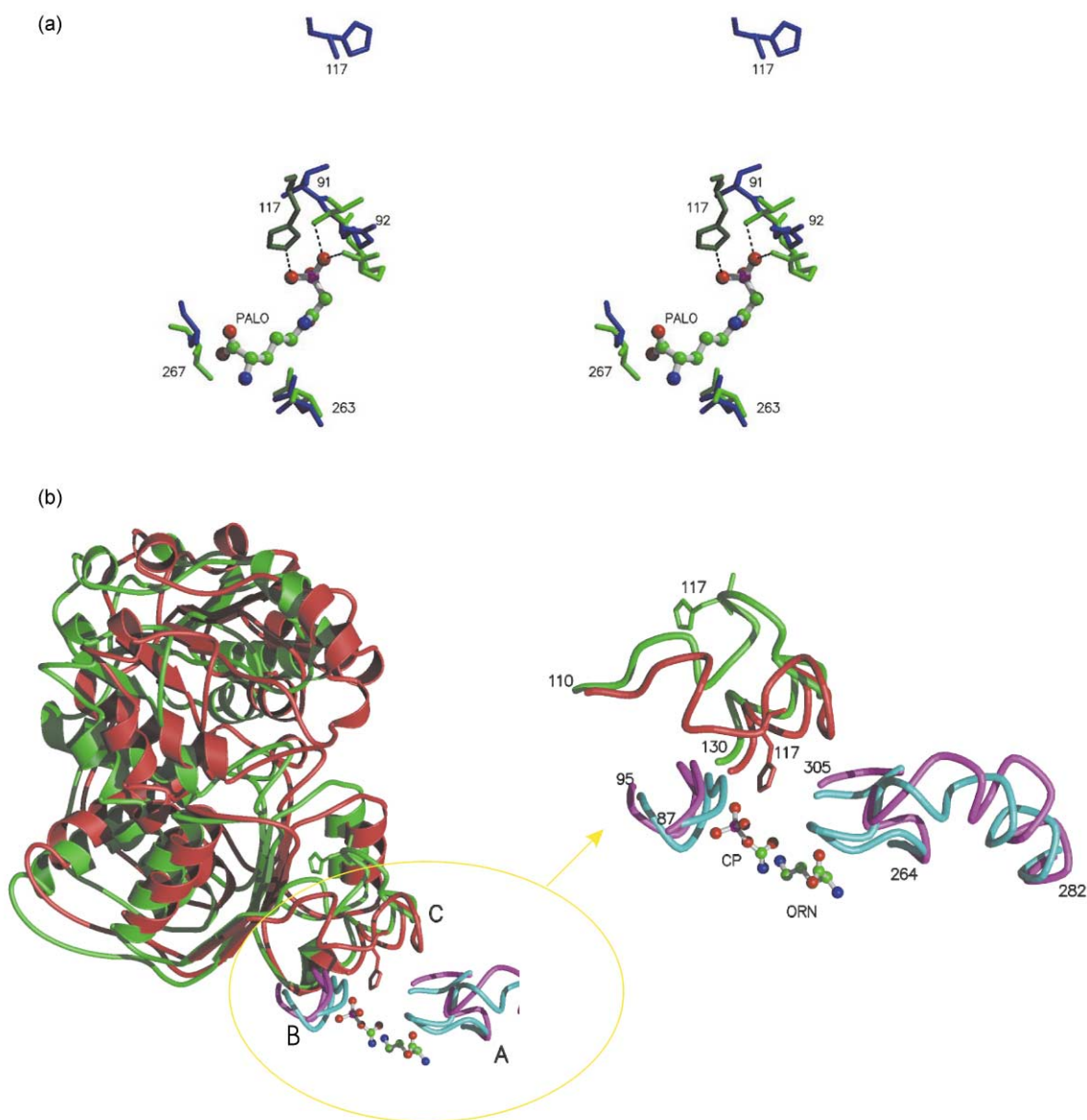


Fig. 3 (A) Superposition of some of the residues that surround the ligand and that are different in the monomer of ovine unliganded OTCase (this paper) and in the human liganded protein.¹¹ δ -PALO bound to the human protein is shown as a ball-and-sticks model. Some of the amino acids surrounding it in the human enzyme are in green (subunit A), whilst His 117, that belongs to another subunit, is in dark green. Contacts of the ligand with the residues shown are indicated by dashed lines. Blue residues represent the position of the same residues in the OTCase of the ovine protein. It is evident that His 117 (dark blue) is now very far from the previous position, owing to the rearrangement that involves the organization of the different subunits. (B) Overall scheme of the conformational rearrangements that take place in the monomer of mammals OTCase, and its consequences on the quaternary structure of the trimer. The position of the two ligands, carbamoyl-P (CP) and ornithine (ORN), is hypothetically derived from the position of δ -PALO. The main chain trace of portion of the subunit to which the co-substrates are bound (regions labelled A and B), are drawn in cyan (liganded) and magenta (unliganded enzyme). The second subunit interacting with carbamoyl-P is drawn in red (liganded) and green (unliganded enzyme). The binding of carbamoyl-P, which interacts with His 117 of the second subunit (the region labelled C), induces the ordering of the main chain from 110 to 124, causing a movement of the entire polypeptide chain and a consequent change at the interface between the two subunits. A secondary effect is the movement of chain from 87 to 95 (labelled B). The binding of the second substrate, ornithine, affects the order of the region from 264 to 282 (labelled A) inducing a conformational modification of the protein limited to the subunit where the co-substrate binds.

conformation. In the model of the human enzyme, the phosphate moiety of δ -PALO directly interacts, among others, with residues from 90 to 93 of the monomer to which it is bound and with His 117 of a symmetry-related one. The region from 90 to 93 assumes a different conformation in the liganded and unliganded state of the protein, whilst residue 117 in our model belongs to a disordered area (Fig. 3A). We can speculate that the binding of carbamoylphosphate with its phosphate group induces a shift of some chains and at the same time fixes a region that is otherwise flexible in the unliganded protein. In doing so, it induces a relative re-orientation of two monomers, since the direct interaction with His 117 pulls all the rest of the polypeptide chain of the symmetry-related monomer. Consequently, these movements become also responsible for the

re-organization of the trimer, since the zones involved in the rearrangement belong to two different monomers of the same trimer (Fig. 3B). Conformational modifications due to the ornithine moiety of the pseudo-substrate are less relevant, since they involve residues located in the same monomer where the ligand is bound.

Similar behavior can be observed comparing the liganded and unliganded models of anabolic OTCase from *E. coli*. The relative displacement of the subunits following the interaction with δ -PALO is less pronounced. This is possibly due to the differences in the residues that interact with the ligand: in particular, the position of His 117 of the human protein is replaced by Gln 82 in the bacterial enzyme. As a consequence, its interaction with the negatively charged group of the bi-substrate

analogue is less tight and the effect after its release less pronounced. The comparison of liganded OTCase from *E. coli*⁹ and the unliganded catabolic OTCase from *Pseudomonas aeruginosa*⁷ have suggested that a relative reorganization of the two domains inside a single subunit are responsible for the allosteric properties of the enzyme. These conclusions were inferred using one enzyme that possesses a dodecameric structure, where the kind of rearrangements we observe cannot take place without a drastic reorganization of the quaternary structure of the dodecamer. Moreover, it is worth noticing also that in bacterial ATCase the quaternary structure is more complex, since the allosteric properties are controlled by some regulatory subunits, distinct from the catalytic ones.

Conclusions

Despite the low resolution data for the structure of the ovine enzyme, the results presented suggest that the conformation of the ovine enzyme can be considered representative of the inactive T-state of an eukaryotic OTCase, whilst the quaternary structures of the human enzyme complexed with carbamoylphosphate¹² and δ -PALO¹¹ correspond or are more close to the active R state. The transition from an inactive to an active conformation of the trimeric enzyme involves a modification of the conformation of some portions of the polypeptide chain involved in the interactions with the substrate(s). These limited movements do not produce drastic conformational changes in the subunit itself, but rather they induce a re-organization of the relative orientation of the quaternary structure, with the three subunits that reorient with respect to each other. The comparison between the liganded and unliganded forms of the enzyme allows speculation about the sequence of the events taking place after the interactions of the proteins with the substrates: the first substrate, carbamoylphosphate, induces a rearrangement among the subunits, thus being responsible for the cooperative behaviour of the enzyme, whilst the second substrate produces minor rearrangements inside a single subunit.

Experimental

Materials

δ -PALO was synthesized and further purified essentially as described by De Martinis *et al.*²⁶ Epoxyactivated Sepharose 6B was obtained from Amersham Biosciences (Uppsala, Sweden). All chemicals used were of analytical grade.

Enzyme purification

Ovine liver from slaughter-age animals was obtained from a local abattoir. The liver samples were stored at $-20\text{ }^{\circ}\text{C}$ until homogenized. All steps of enzyme purification were carried out at $4\text{ }^{\circ}\text{C}$, except for adsorption and elution from δ -PALO-Sepharose 6B. All buffers contained 2 mM 2-mercapto-ethanol and 1 mM EDTA. Defrosted portions of liver (4 g) were homogenized in a Potter homogenizer in 10 mM Tris-HCl, pH 7.4, (buffer A), containing 0.5% (w/v) Triton X-100 (16 mL). After centrifugation, the supernatant containing OTCase activity was separated from the upper fat pad by filtration through glass wool. The crude extract was mixed with the affinity adsorbent (δ -PALO-Sepharose 6B), equilibrated in buffer A, and incubated in bath for 40 min at $27\text{ }^{\circ}\text{C}$. After washing with buffer A followed by washing with buffer A containing 100 mM KCl (buffer B), the enzyme was eluted with 10 mM carbamoylphosphate in buffer A and stored at $-20\text{ }^{\circ}\text{C}$ in 25 mM sodium phosphate, pH 7.7. The partially purified enzyme preparations were pooled, concentrated and, after phosphate removing by a PD-10 Sepharose G-25 column, applied to a $2.5 \times 6\text{ cm}$ δ -PALO affinity column, equilibrated in buffer A. After washing with 2 column volume (CV) of buffer A and 2 CV of buffer

B, the enzyme was eluted with 2 CV of 10 mM carbamoylphosphate in buffer A. The purified enzyme was dialyzed, concentrated and stored at $-20\text{ }^{\circ}\text{C}$ in 25 mM sodium phosphate, pH 7.0 buffer containing 10 mM carbamoylphosphate and 25 mM L-norvaline. In these conditions, purified ovine ornithine transcarbamoylase was stable for months, without loss of activity.

Protein concentrations were determined by measurement of A_{280} or according to ref. 27. Ornithine transcarbamoylase activity was determined according to the procedure of Ceriotti and Gazzaniga²⁸ modified as previously described.¹⁵ One unit of enzyme catalyzes the formation of $1\text{ }\mu\text{mol min}^{-1}$ of L-citrulline at $37\text{ }^{\circ}\text{C}$.

Thermal stability assay

Thermal stability was measured by incubating the enzyme ($22\text{ }\mu\text{g}$ per $240\text{ }\mu\text{L}$) at a given temperature in 0.051/0.1/0.051 M diethanolamine/MES/N-ethylmorpholine, pH 8.6, 2 mM 2-mercapto-ethanol, in the absence or in the presence of saturating concentration of ligand(s). Aliquots ($10\text{ }\mu\text{L}$) were removed at intervals and after rapid cooling to $25\text{ }^{\circ}\text{C}$ assayed for residual activity, which was expressed as a percentage of initial activity. From the semi-logarithmic plots of the inactivation kinetics, the $t_{1/2}$ (time required for the activity to drop to half of its initial value) was determined for each set of experimental conditions.

Protein sequencing

The N-terminal sequence of purified OTCase was determined by adsorptive biphasic column technology, using an HPG1000 A protein sequenator (Hewlett-Packard) with the routine 3.0 method and PHT_4M HPLC method.

Thiol groups analysis

Free thiol groups were determined using the Ellman's reagent, according to ref. 29. The purified protein (7 nmol monomer) was incubated with 8 M urea, reacted with Ellman's reagent [5,5'-dithiobis(2-nitrobenzoic acid)] (DTNB), and the increase in absorbance monitored at 412 nm $\epsilon_{412}\text{ }13\text{ }600\text{ M}^{-1}\text{ cm}^{-1}$. The final concentration of DTNB was 1.25 mM; the reaction buffer was 100 mM sodium phosphate, pH 8; the final volume was 1 mL.

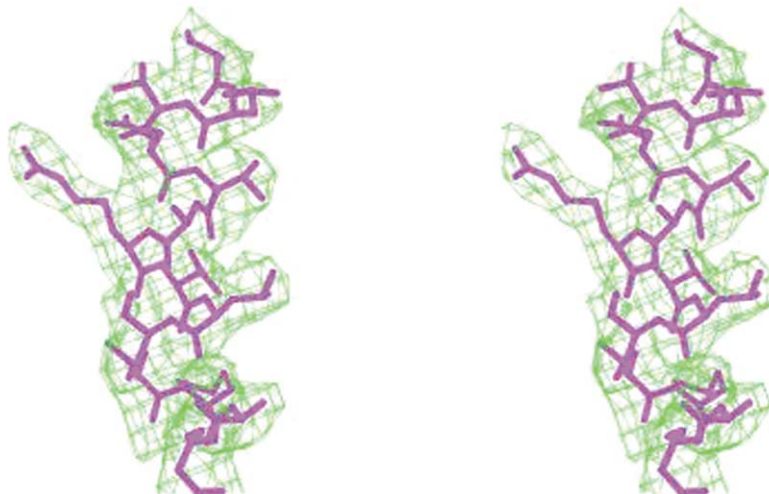
Total thiol groups were determined according to ref. 30. The protein (10 nmol monomer) was incubated with 8 M urea, reacted with 50 mM labeled (14C) iodoacetic acid ($50\text{ }\mu\text{Ci }\mu\text{mol}^{-1}$ specific activity) and digested for 12 h with TPCK-trypsin (1:20) at room temperature. The tryptic peptides were separated by RP-HPLC on a Phenomenex C18 column ($150 \times 4,60\text{ mm}$ id, particle size 5 μm) using 0.05% trifluoroacetic acid as an aqueous solvent (solvent A) and 0.05% trifluoroacetic acid in acetonitrile (CH_3CN), as solvent B. A linear gradient, (0–50% of B in 80 min), was applied at a flow rate of 0.7 mL min^{-1} . The eluate was monitored at 214 nm and the individual peaks were collected manually. Aliquots of individual peaks were counted for radioactivity.

Crystallization

The protein was concentrated with ultrafiltration devices (Centricon YM-10, Millipore Corporation, Bedford, MA USA) with a molecular cut-off of 10 kDa, up to a final concentration of about $7\text{--}9\text{ mg mL}^{-1}$. Crystals were obtained using the vapor diffusion method (hanging and sitting drop). $2\text{--}3\text{ }\mu\text{L}$ of protein solution, 10 mM Tris-HCl, pH 7.4, were mixed with an equal volume of a solution containing sodium acetate 0.1 M, 8% (w/v) PEG 4000, pH 4.6 and equilibrated against the same precipitant solution. Cubic shaped crystals, the largest having dimensions of about 0.2 mm, grew in a few days. Crystals belong to $P4_332$ space group, with $a = b = c = 184.7\text{ \AA}$. The

Table 4 Statistics on data collection and processing. A total of 139 662 reflections were measured, with an overall multiplicity of 10

Resolution interval	No. of independent reflections	Completeness	Multiplicity	$\langle I/\sigma(I) \rangle$	R_{merge}
∞ –7.80	1359	97.1	9.4	16.4	0.036
7.80–5.53	2304	98.3	10.0	7.6	0.097
5.53–4.52	2935	99.0	10.2	6.3	0.117
4.52–3.92	3462	99.8	10.2	4.4	0.171
3.92–3.51	3877	99.5	10.0	2.3	0.322

**Fig. 4** A detail of the electron density around residues 123–136. Maps were calculated with coefficients $|2F_{\text{obs}} - F_{\text{calc}}|$ and phases from the model. The contouring level is at 1σ .

subsequent structural determination has shown that the asymmetric unit contains one monomer, corresponding to a V_M of $7.3 \text{ \AA}^3 \text{ Da}^{-1}$ and a solvent content of *ca.* 80%. The extremely high solvent content partially explains the fact that crystals, despite their reasonable size, do not diffract at all under a rotating anode X-ray source and diffract to only 3.5 \AA resolution with synchrotron radiation.

Data collection and processing

Data were collected at the single crystal diffraction beam-line of the Elettra synchrotron in Trieste (Italy). Before mounting, the crystal was soaked for about 20 s in a cryo-protectant solution, prepared by mixing the mother liquid of the crystal with 30% glycerol. An entire data set was measured from one crystal, using a wavelength of 1.05 \AA and a crystal-to-detector distance of 400 mm. 48 frames of 0.9° rotation each gave a 99 per cent complete data set. Data were processed with MOSFLM and merged with SCALA.³¹ Statistics on data collection and processing are reported in Table 4.

Structure solution and refinement

The structure was solved by using the molecular replacement technique, with the program AMoRe.³² One monomer of the model of holo-OTCase from *E. coli* (PDB code 2OTC⁹) was selected as the starting model, since at that time the coordinates of the human enzyme¹¹ were not yet available. This model was modified according to the amino acid sequence of the human enzyme and its conformation minimised. Since the protein had been purified in the presence of carbamoylphosphate, L-norvaline and phosphate, we decided to use the holo model of the bacterial protein. This choice did not influence the final result, as the final solution revealed that only one monomer is present in the asymmetric unit and the trimer was generated by symmetry operations. The highest maximum of the rotation function was used to orient the molecule, which was then subjected to a translation function.³² In the crystal cell, the monomer is positioned close to a crystallographic three-fold axis, in such a way that a crystallographic OTCase trimer was

generated. The search for a second molecule was unsuccessful, and in fact the presence of one polypeptide chain in the asymmetric unit gives rise to a self-contained packing, despite the extremely large solvent content. The structure was refined using simulated annealing and energy minimization procedures, performed with the computer package CNS,³³ alternated with manual rebuilding using the program O.³⁴ Since the first 54 amino acids of the sequence are 98% conserved in comparison with the human enzyme, as well as the number of cysteine residues, a large similarity with the human protein was assumed also for the rest of the chain and the sequence of the human protein was used in the course of refinement. This is also justified by the large degree of conservation of this family of proteins, especially in mammals.³⁵ Owing to the low resolution of the maps, no solvent molecules were inserted, with the exception of two, located quite close to amino acid side chains and refined to a very low B factors. We cannot rule out the possibility that these positions could represent side chains that are different in the ovine protein with respect to the human protein.

The final structure consists of 2504 protein atoms and 11 ligand atoms, for a final crystallographic R factor of 0.21 ($R_{\text{free}} = 0.25$). Details on the refined model are reported in Table 5.

Quality of the model

Cubic crystals of ovine OTCase diffract to a maximum resolution of 3.5 \AA , despite their reasonable size and the use of an X-ray beam of a third-generation synchrotron. This can be ascribed to the loose crystal packing and to the unusually high solvent content. However, the low protein content has the advantage that the ratio observations/variables (*ca.* 1.8) is higher than that expected for a structure solved at this resolution with an average solvent content and this makes the refined molecular model slightly more reliable than might be expected. The electron density is well defined (Fig. 4), with the exception of two disordered regions previously described. The geometry of the final model is satisfactory for a 3.5 \AA resolution structure: an analysis performed with PROCHECK³⁶ indicates

that all the geometrical parameters examined are better than expected for a structure at this resolution.

Coordinates. The molecular model has been deposited at the Brookhaven Protein Data Bank (accession number 1FB5).

Abbreviations

OTCase: ornithine transcarbamoylase; ATCase: aspartate transcarbamoylase; δ -PALO: δ -N-(phosphonacetyl-L)-ornithine; Carbamoyl-P: carbamoylphosphate; V_M : crystal volume per unit of protein molecular mass; EDTA: Ethylenediamine-tetraacetic acid; SDS-PAGE: sodium dodecyl-sulfate polyacrylamide gel electrophoresis; MES: 2-(N-morpholino)ethanesulfonic acid; DTNB: 5,5'-dithiobis(2-nitrobenzoic acid); RP-HPLC: reversed phase-high pressure liquid chromatography

Acknowledgements

The technical support of the CNR staff at the X-ray diffraction beam-line of Elettra is gratefully acknowledged. The authors also wish to thank Dr L. Chiarelli (Dipartimento di Biochimica, Università di Pavia, Italy) and Dr B. Casado (Department of Medicine, Georgetown University, Washington D. C., USA) for skilful technical assistance in the determination of thiol groups. This work was partially supported by the Ministero per l'Istruzione, l'Università e la Ricerca Scientifica (MIUR), and the Italian National Research Council (C. N. R.), Rome.

References

- 1 A. L. Horwich, W. A. Fenton, K. R. Williams, F. Kalousek, J. P. Kraus, R. F. Doolittle, W. Konigsberg and L. E. Rosenberg, *Science (Washington, D. C.)*, 1984, **224**, 1068–1074.
- 2 C. Legrain, P. Halleux, V. Stalon and N. Glansdorff, *Eur. J. Biochem.*, 1972, **27**, 93–102.
- 3 M. Penninckx, J. P. Simon and J. M. Viame, *Eur. J. Biochem.*, 1974, **49**, 429–442.
- 4 T. A. Hoover, W. D. Roof, W. D. Foltermann, G. A. O'Donovan, D. A. Bencini and J. R. Wild, *Proc. Natl. Acad. Sci. U. S. A.*, 1983, **80**, 2462–2466.
- 5 W. H. Konigsberg and L. Henderson, *Proc. Natl. Acad. Sci. U. S. A.*, 1983, **80**, 2467–2471.
- 6 W. N. Lipscomb, *Adv. Enzymol. Relat. Areas Mol. Biol.*, 1994, **68**, 67–151.
- 7 V. Villeret, C. Tricot, V. Stalon and O. Dideberg, *Proc. Natl. Acad. Sci. U. S. A.*, 1995, **92**, 10762–10766.
- 8 V. Villeret, B. Clantin, C. Tricot, C. Legrain, M. C. Roovers, V. Stalon, N. Glansdorff and J. van Beeumen, *Proc. Natl. Acad. Sci. U. S. A.*, 1998, **95**, 2801–2806.
- 9 L. Jin, B. A. Seaton and J. F. Head, *Nat. Struct. Biol.*, 1997, **4**, 622–625.
- 10 Y. Ha, M. T. McCann, M. Tuchman and N. M. Allewell, *Proc. Natl. Acad. Sci. U. S. A.*, 1997, **94**, 9550–9555.
- 11 D. Shi, H. Morizono, Y. Ha, M. Aoyagi, M. Tuchman and N. M. Allewell, *J. Biol. Chem.*, 1998, **273**, 34247–34254.
- 12 D. Shi, H. Morizono, X. Yu, L. Tong, N. M. Allewell and M. Tuchman, *Biochem. J.*, 2001, **354**, 501–509.
- 13 A. W. Miller and L. C. Kuo, *J. Biol. Chem.*, 1990, **265**, 15023–15027.
- 14 A. De Gregorio, A. Risitano, C. Capo, C. Crinò, R. Petruzzelli and A. Desideri, *Biochem. Mol. Biol. Int.*, 1999, **47**, 965–970.
- 15 F. Kalousek, B. Francois and L. E. Rosemberg, *J. Biol. Chem.*, 1978, **253**, 3939–3944.
- 16 G. Valentini, A. De Gregorio, C. Di Salvo, R. Grimm, E. Bellocco, G. Cuzzocrea and P. Iadarola, *Eur. J. Biochem.*, 1996, **239**, 397–402.
- 17 M. Marshall and P. P. Cohen, *J. Biol. Chem.*, 1972, **247**, 1641–1653.
- 18 C. J. Lusty, R. L. Jilka and E. H. Nietsch, *J. Biol. Chem.*, 1979, **254**, 10030–10036.
- 19 U. K. Leammy, *Nature (London)*, 1970, **227**, 680–685.
- 20 A. De Gregorio, G. Valentini, E. Bellocco, A. Desideri and G. Cuzzocrea, *Comp. Biochem. Physiol.*, 1993, **105B**, 497–501.
- 21 L. C. Kuo, W. Herzberg and W. N. Lipscomb, *Biochemistry*, 1985, **24**, 4754–4761.
- 22 P. J. Snodgrass, *Biochemistry*, 1968, **7**, 3047–3051.
- 23 H. Morizono, M. Tuchman, S. Rajagopal, M. T. McCann, C. D. Listrom, X. Yuan, D. Venugopal, G. Barany and N. M. Allewell, *Biochem. J.*, 1997, **322**, 625–631.
- 24 M. Tuchman, H. Morizono, O. Reish, X. Yuan and N. M. Allewell, *J. Med. Genet.*, 1995, **32**, 680–688.
- 25 X. Xiong and P. M. Anderson, *Arch. Biochem. Biophys.*, 1989, **270**, 198–207.
- 26 M. L. De Martinis, P. Mc Intyre and N. Hoogenraad, *Biochem. Int.*, 1981, **3**, 371–378.
- 27 O. H. Lowry, N. J. Rosebrough, A. Farr and R. J. Randall, *J. Biol. Chem.*, 1951, **193**, 265–275.
- 28 G. Ceriotti and A. Gazzaniga, *Clin. Chim. Acta*, 1966, **14**, 57–62.
- 29 P. W. Riddles, R. L. Blakely and B. Zerner, *Meth. Enzymol.*, 1983, **91**, 49–60.
- 30 R. P. Swenson, C. H. Jr Williams, V. Massey, S. Ronchi, L. Minchiotti, M. Galliano and B. Curti, *J. Biol. Chem.*, 1982, **257**, 8817–8823.
- 31 Collaborative computational project no. 4, *Acta Crystallogr.*, 1994, **D50**, 760–763.
- 32 J. Navaza, *Acta Crystallogr.*, 1994, **A50**, 157–163.
- 33 A. T. Brünger, P. D. Adams, G. M. Clore, W. L. DeLano, P. Gros, R. W. Grosse-Kunstleve, J.-S. Jiang, J. Kuszewski, N. Nilges, N. S. Pannu, R. J. Read, L. M. Rice, T. Simonson and G. L. Warren, *Acta Crystallogr.*, 1998, **D54**, 905–921.
- 34 A. T. Jones, Y.-J. Zou, S. W. Cowan and M. Kielgaard, *Acta Crystallogr.*, 1991, **A47**, 110–119.
- 35 J. P. Kraus, P. E. Hodges, C. L. Williamson, A. I. Horwich, F. Kalousek, K. R. Williams and L. E. Rosemberg, *Nucleic Acids Res.*, 1985, **13**, 943–952.
- 36 R. A. Laskowski, M. W. McArthur, D. S. Moss and J. Thornton, *J. Appl. Crystallogr.*, 1993, **26**, 283–291.